

We are IntechOpen, the world's leading publisher of Open Access books Built by scientists, for scientists

6,900

Open access books available

186,000

International authors and editors

200M

Downloads

Our authors are among the

154

Countries delivered to

TOP 1%

most cited scientists

12.2%

Contributors from top 500 universities



WEB OF SCIENCE™

Selection of our books indexed in the Book Citation Index
in Web of Science™ Core Collection (BKCI)

Interested in publishing with us?
Contact book.department@intechopen.com

Numbers displayed above are based on latest data collected.
For more information visit www.intechopen.com



Transient Effectiveness Methods for the Dynamic Characterization of Heat Exchangers

Tianyi Gao, Bahgat Sammakia and James Geer

Additional information is available at the end of the chapter

<http://dx.doi.org/10.5772/67334>

Abstract

This chapter introduces transient effectiveness methods for dynamic characterization of heat exchangers. The chapter provides a detailed description and review of the transient effectiveness methodology. In this chapter, all the transient effectiveness-related knowledge/works are summarized. The goal of this chapter is to provide a thorough understanding of the transient effectiveness for the reader and to provide guidance for utilizing this methodology in related heat exchanger transient characterization studies. Basically, there are three important applications for transient effectiveness methodology: (1) characterization of heat exchanger dynamic behaviors; (2) characterization of the transient response of closed-coupled cooling/heating systems with multiple heat exchanger units; and (3) development of compact transient heat exchanger models. This innovative modeling method can be used to assist in the development of physics-based predictive, capabilities, performance metrics, and design guidelines, which are important for the design and operation of highly reliable and energy efficient mechanical systems using heat exchangers.

Keywords: transient effectiveness, inlet temperature variation, fluid mass flow rate variation, heat exchanger dynamic performance, compact transient modeling, system level characterization

1. Introduction

Transient effectiveness methodology is a new analytical method which is developed for studying the dynamic performance of a heat exchanger. The concept was originally introduced by Cima and London in 1958 and used as a signature in representing the heat exchanger transient performance. The concept was then used for developing generalized transient effectiveness for plotting the transient response of a counter-flow heat exchanger [1]. In some of the recent

studies [2, 3], the transient effectiveness concept is used for developing a new methodology for dynamic characterization of cross-flow heat exchangers. In this chapter, a complete summary and review of the transient effectiveness method is provided, including the methodology development, transient effectiveness characterization, modeling validation, as well as the three major application and usefulness of the transient effectiveness. The heat exchanger configuration considered in most of the studies as well as in this chapter is an unmixed-unmixed cross flow one. It needs to be mentioned here that the majority of the work and results are summarized and published in different scientific journals by the same group of authors. This work provides a complete connection of all the existing research efforts and major results related to the transient effectiveness methodology. The readers can obtain a clear idea of this methodology and utilize it in the corresponding research and studies directly.

2. Transient effectiveness

2.1. Governing equations and numerical solution

Effectiveness which is defined as the ratio of actual heat transferred rate over the maximum heat transfer rate is introduced for characterizing heat exchanger steady-state performance. Cima and London [1] extended this concept to a time-dependent one in [1]. In their study, a generalized transient effectiveness was developed based on Eqs. (1a) and (1b), and then used as a means for representing the transient analog results for a counter-flow heat exchanger instead of using outlet temperatures.

$$\varepsilon_h(t) = \frac{c_{p_h}[T_{h,in}(t) - T_{h,out}(t)]}{c_{p_{\min}}[T_{h,in}(t) - T_{c,in}(t)]} \quad (1a)$$

$$\varepsilon_c(t) = \frac{c_{p_c}[T_{c,out}(t) - T_{c,in}(t)]}{c_{p_{\min}}[T_{h,in}(t) - T_{c,in}(t)]} \quad (1b)$$

The transient effectiveness concept and its governing equations were introduced and directly used for characterizing dynamic performance of a cross-flow heat exchanger in references [2, 3]. In these studies, the transient effectiveness governing equations are solved numerically by coupling them with thermal dynamic heat exchanger equations which are shown in Eqs. (2)–(4). These three sets of governing equations are widely used in most of the existing literature [4–9] for solving similar problems. A full numerical solution for these equations and a comprehensive heat exchanger transient behavior characterization using numerical modeling are conducted in [10–13]. Most of the variation scenarios were covered in these studies, including single fluid temperature variations, fluid mass flow rate variations, as well as multiple variation combinations.

$$\frac{\partial T_{wall}}{\partial t} = r_c^\beta \cdot T_c + R \cdot r_h^\beta \cdot T_h - (r_c^\beta + R \cdot r_h^\beta) \cdot T_{wall} \quad (2)$$

$$V_c \frac{\partial T_c}{\partial t} = r_c^\beta \cdot T_{wall} - r_c^\beta \cdot T_c - r_c \frac{\partial T_c}{\partial X} \quad (3)$$

$$\frac{V_h}{R} \frac{\partial T_h}{\partial t} = r_h^\beta \cdot T_{wall} - r_h^\beta \cdot T_h - r_h \frac{\partial T_h}{\partial Y} \quad (4)$$

2.2. Transient effectiveness method verification

The methodology and the numerical solution are verified by comparison with several published results in [1, 14, 15]. First, several published analytical solutions and analog solutions for the transient effectiveness of a 1D contour-flow heat exchanger are used [14]. The equivalent method was used and the same transient effectiveness equations were integrated into the numerical code and then compared to the results presented in a form as generalized transient effectiveness. **Figure 1(a)** shows a comparison of the numerical solutions and the analytical data points [14, 15]. This case represents a response of a heat exchanger under a fluid

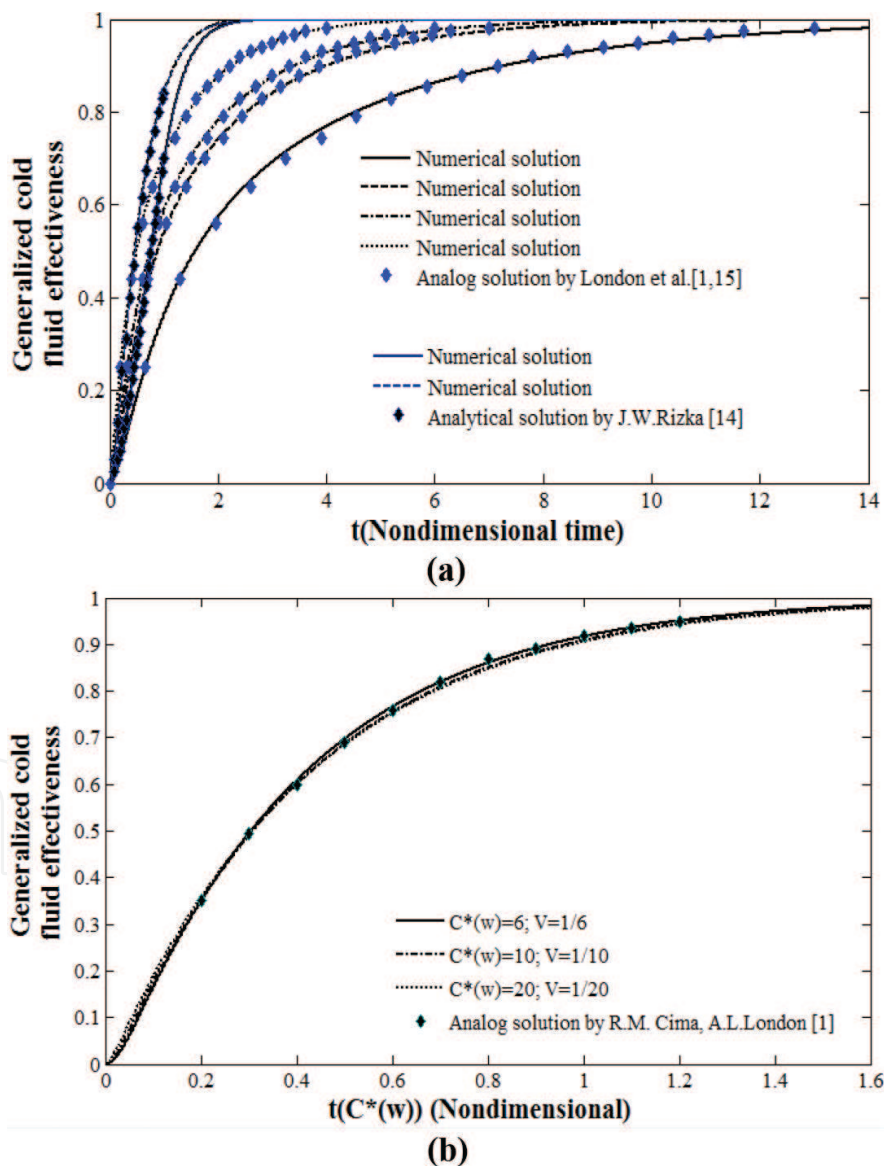


Figure 1. (a) Comparison of the numerical solutions with the analytical results in [14] and analog results in [1, 15]; (b) Comparison of the numerical solutions with the analog results in [1] for NTU 1–1.5 and NTU 1.5–1.

inlet temperature step change. **Figure 1(b)** shows comparison between the analog solution [1] and numerical solution under a step change in the fluid mass flow rate. The mass flow rate step increase results in the NTU variation from 1 to 1.5, and the step decrease results in the NTU variation from 1.5 to 1, which is also mentioned in the figure caption. It can be seen from both figures that the results are in good agreement, and different scenarios including fluid mass flow rate change and inlet temperature change are validated.

2.3. Parametric study

A detailed study of the characterizing transient effectiveness under different variation conditions including both inlet temperature change and mass flow rate change is presented in [2, 3]. It is found in these studies that the transient effectiveness can be used as a measure of the heat exchanger dynamic performance from one steady state to the new equilibrium state under certain inputs. In addition, the impact of modeling physical parameters, including NTU , E , R , and V , can be represented on the effectiveness curves. NTU results are chosen as an example to discuss in this section. More detailed parametric results are summarized in references [2, 3].

2.3.1. Inlet temperature variation

The inlet temperature variation does not influence the final steady-state values of the effectiveness curve lines. This means that the effectiveness curve always returns to the initial value after a certain transient variation. **Figure 2** shows the transient effectiveness of two fluids plotted versus nondimensional time for a wide range of NTU values for the step change. It can be seen from the figure that NTU governs both transient and steady-state variation of effectiveness. The larger the NTU value, the longer time is taken to reach the final steady state. When comparing the hot fluid transient effectiveness curve and the cold fluid transient effectiveness curve, a time lag is seen on the hot fluid curves. This time lag indicates that the corresponding fluid takes some time to begin to respond at the outlet, after the variation is applied at the inlet.

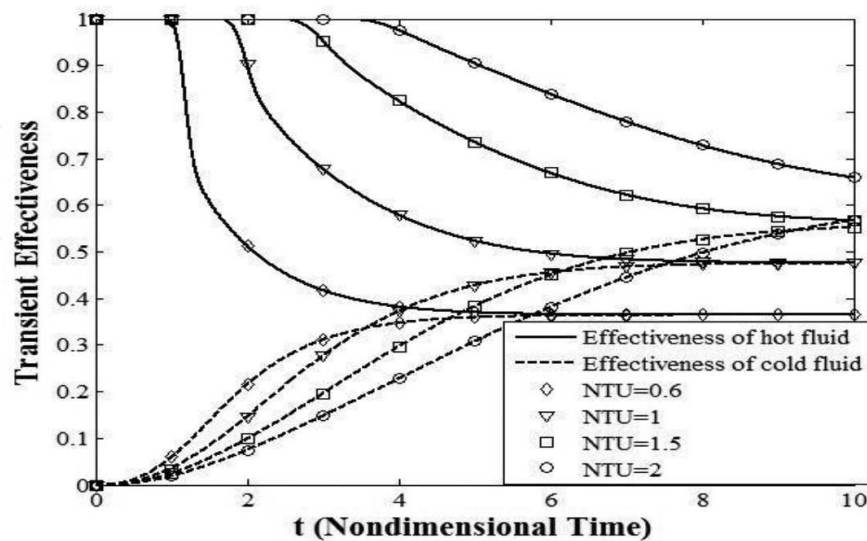


Figure 2. Effect of NTU on the transient effectiveness results with $E = 1$, $V_h = V_c = 1$, $R = 1$; step change to the hot fluid inlet temperature.

The larger the NTU value, the longer the time lag. A larger NTU value can be simply understood as a larger heat exchanger physical size. Therefore, the time lag is longer for a larger NTU value.

2.3.2. Fluid mass flow rate variation

The characteristics of the effectiveness under fluid mass flow rate change are discussed in this section. **Figure 3** shows that the steady-state conditions of the effectiveness curve changes due to a change in fluid mass flow rate. The difference is clearly seen from the transient effectiveness between a cold fluid mass flow rate change and a hot fluid mass flow rate change.

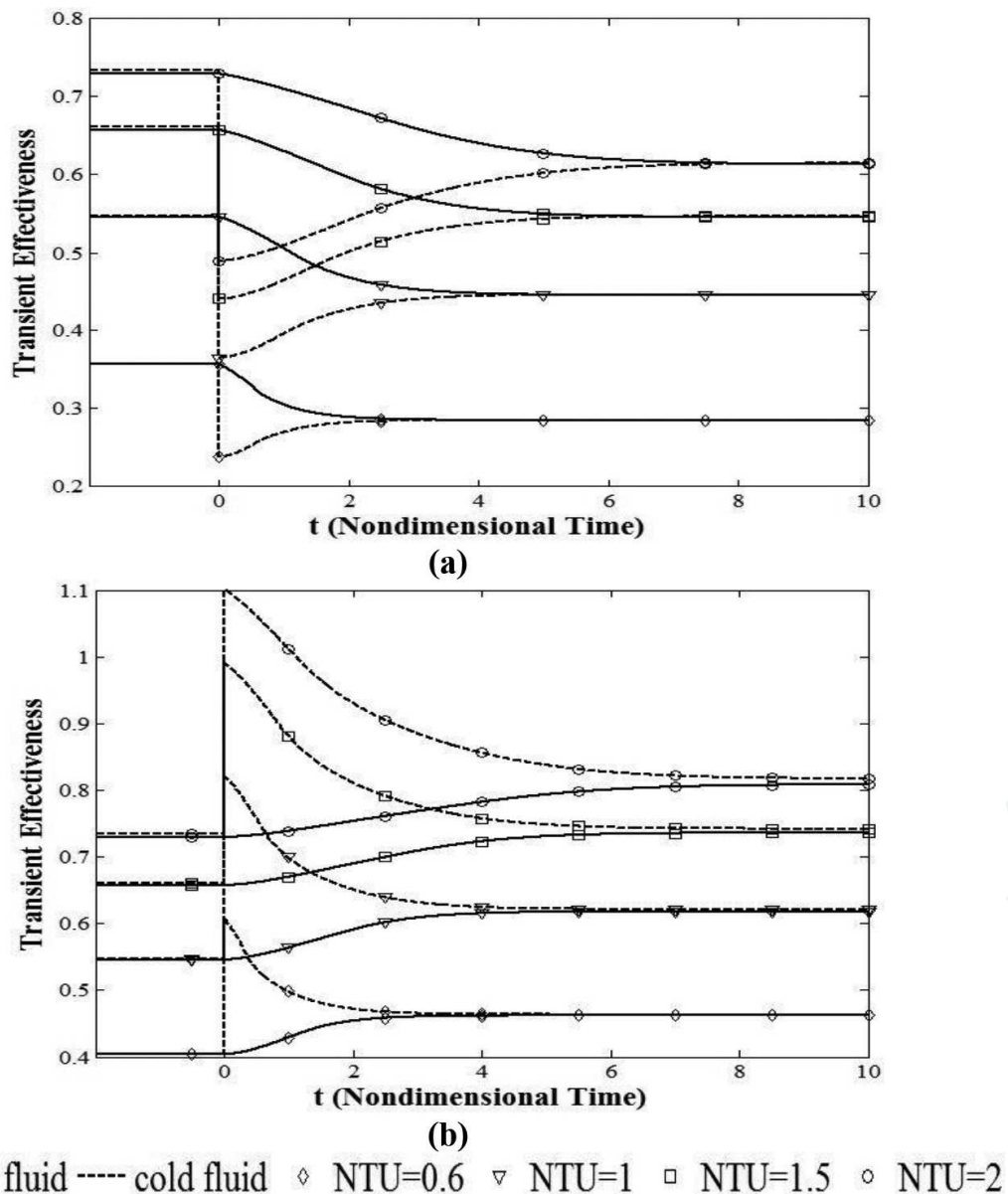


Figure 3. Effect of NTU on the transient effectiveness results with $E = 0.5$, $R = 1$, $V = 1$; (a) step change to hot fluid mass flow rate; (b) step change to cold fluid mass flow rate.

A step change is seen in all the cold fluid curves before the curves move smoothly and reach a steady state. In Eq. (1b), $T_{c,out}(t)$, and C_c/C_{\min} (C_{\min} is considered as a hot fluid capacity rate, which gives $C_c/C_{\min} = E$) govern the cold fluid effectiveness variations. The previously mentioned step change at the very beginning is due to the step change of $C_c(E)$. In terms of a mass flow rate ramp variation scenario, the variation in transient effectiveness curves at the beginning is dominated by E and $T_{c,out}(t)$. The transient effectiveness also illustrated the combination impact of the fluid mass flow rate variation and the physical parameters. As an example, **Figure 3** shows the transient effectiveness results versus different NTU values. The impact of the NTU value on the steady-state and transient performance of the transient effectiveness can be clearly seen in the curves of the figure. As an example, the larger the NTU value the longer time the heat exchanger takes to reach steady state. The difference of the variation of the cold fluid and the hot fluid is clearly distinguished in the same figure.

It can be seen that the transient effectiveness curves are able to represent the transient response of heat exchangers under different variation conditions by comparing the curves shown in **Figure 3(a)** and **(b)**. This means that a transient effectiveness curve represents more physical information than an outlet temperature curve, since the curves are distinguished clearly when different boundary conditions are applied. In addition, the transient effectiveness curves also reflect the influences of the physical parameters on the transient and steady-state responses of the heat exchangers.

2.4. Experimental verification

Experimental measurements on a liquid to air cross-flow heat exchanger cores are presented in reference [16], in which the liquid mass flow rate or inlet temperature varied in time following controlled functional forms (step jump and ramp). The specific design enables the control of transient variations in the inlet temperature and mass flow rate on both the air and water flow streams supplied to the heat exchanger device. More details regarding the entire experimental setup and tests can be found in reference [16]. The experimental data were used to characterize and validate the transient effectiveness methodology and the transient numerical solution in reference [17], and the more comprehensive understanding of the characteristics of the transient effectiveness is obtained.

For modeling a specific heat exchanger, the modeling physical parameters (E , NTU , R , V_h , V_c) need to be extracted and calculated using the heat exchanger hardware data and one set of steady-state experimental data for modeling a specific heat exchanger and specific dynamic physical scenarios. The procedure can be interpreted as integrating the hardware data into the nondimensional mathematical model (Eqs. (2)–(4)) to model a specific heat exchanger device. One of the methodologies can be referenced to calculate the physical parameter and is presented in reference [18].

2.4.1. Inlet temperature variation

Several functional forms are designed to vary the water inlet temperature and water flow rate. Ramp functions for water inlet temperature change and step functional forms of water flow rate change are selected to present here. The detailed information of each experimental case

designed is shown in **Table 1**. The physical parameters used in the numerical solution for each case are also summarized in **Table 1**.

Water inlet temperature change (°C)	Water flow rate (GPM)	Air flow rate (m ³ /s)	Air inlet temperature (°C)	<i>E</i>	<i>NTU</i>	<i>R</i>	<i>V_{water}</i>	<i>V_{air}</i>
Case 1: Ramp change 22.22–50.28	2	0.2787	22.85	1.62	0.2613	4.78	1.456	0.01
Case 2: Ramp change 23.06–50.26	2	0.3716	23.06	1.2153	0.2186	4.344	1.456	0.01
Water flow rate change (GPM)	Air flow rate (m ³ /s)	Water inlet temperature (°C)	Air inlet temperature (°C)	<i>E</i>	<i>NTU</i>	<i>R</i>	<i>V_{water}</i>	<i>V_{air}</i>
Case 3: Step function 2–5	0.2870	50.40	20.95	1.62	0.264	4.78	1.456	0.01
Case 4: Step function 2–5	0.5574	50.39	21.74	0.79	0.211	3.77	1.456	0.01

Table 1. Test cases.

Two important characteristics of the transient effectiveness are discussed in this section. In case 1, the water inlet temperature is lower than the air inlet temperature at the beginning, and then becomes the hot fluid after the variation. This is the scenario that the cold fluid becomes the hot fluid due to the temperature change. When plotting the transient effectiveness curves, a mathematical singularity point is seen. In Eqs. (1a) and (1b), the term $T_{h,in} - T_{c,in}$ will vary from a positive value to a negative value. This performance is characterized by both simulation modeling and experimental testing. By comparing with the regular fluid temperature curve, the transient effectiveness curves can capture this special scenario. At the same time, they contain all the steady-state and transient characteristics. In case 2, since the water and air are at the same temperature, no singularity point is generated. By comparing the results of cases 1 and 2, the difference between the boundary conditions applied and the transient response is clearly reflected on the transient effectiveness curves. The initial conditions of case 2 can be considered as an idle condition. When plotting the transient effectiveness curve for this special case, there will be a sensitive region after the variation is applied at the time between 10 and 15 s, which is shown in **Figure 5**. Since the two fluid inlet temperatures are same, the numerator and denominator in Eqs. (1a) and (1b) equal 0. Then, even a very minor error in either temperature data may result in a major difference in the effectiveness value. In both **Figures 4** and **5**, the numerical results show a faster response than the experimental results. This is because axial dispersion and longitudinal conduction are neglected in the numerical modeling. When using the transient effectiveness curve plotting the fluid inlet temperature variation cases, the variation form and some of the corresponding characteristics in the fluid inlet temperature can be represented at the same time.

2.4.2. Mass flow rate variation

In cases 3 and 4, variations are applied to the water fluid mass flow rate. **Figures 6** and **7** show the transient effectiveness results of these the two cases, respectively. In terms of the steady-state results, the increase in the water (C_{max} fluid) leads to an increase in the effectiveness value, which is shown in **Figure 6**. In case 4, a special scenario is considered in which the

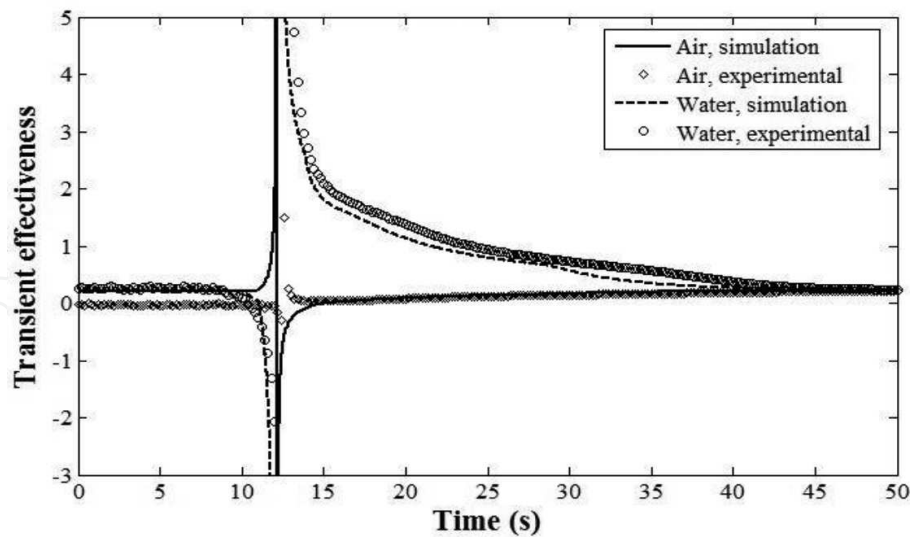


Figure 4. Transient effectiveness results of case 1.

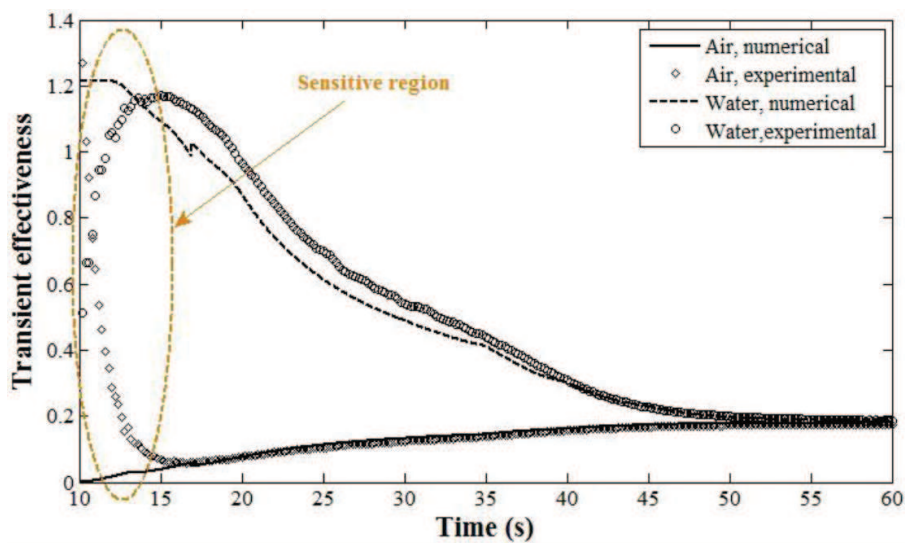


Figure 5. Transient effectiveness of case 2.

minimum capacity fluid (water) becomes the maximum capacity fluid, due to the change in the fluid mass flow rate. Then the air becomes the minimum capacity fluid due to the change. This scenario may be seen in an actual heat exchanger industrial application, especially in certain failure scenarios. It can be seen in **Figure 7** that step changes are seen on both of the curves, before the curves move smoothly and reach the final steady state. By comparing the results shown in **Figures 6** and **7**, it can be found that the transient effectiveness results are clearly different when different fluid mass flow rate variation scenarios are applied. Again, this transient effectiveness methodology can present the heat exchanger dynamic performance in a more comprehensive manner in fluid mass flow rate variation scenarios. It contains the information of the two fluids dynamic responses, and the corresponding variations applied as well (both the fluid inlet temperature and the fluid mass flow rate).

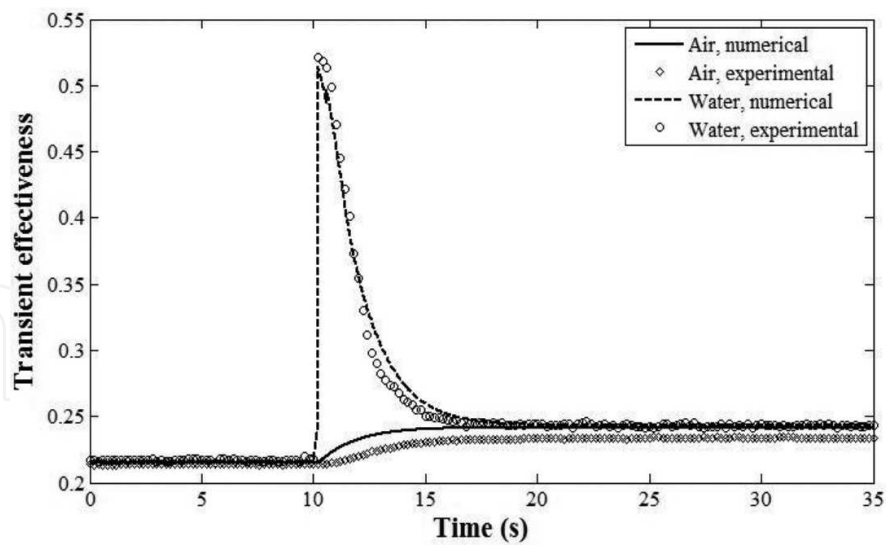


Figure 6. Transient effectiveness results of case 3.

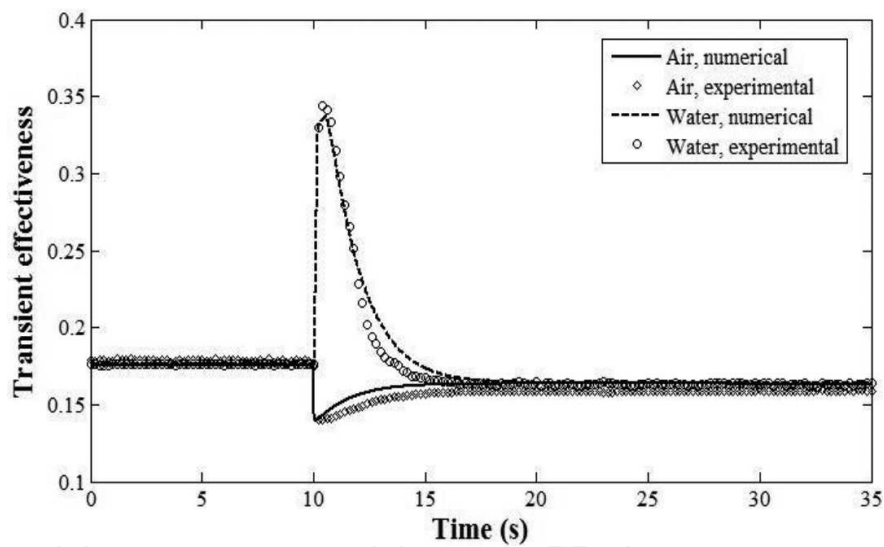


Figure 7. Transient effectiveness results of case 4.

2.4.3. Summary

This section provides several important characteristics of the transient effectiveness for dynamic characterization of a heat exchanger transient performance. Several experimental test cases are selected and analyzed. Two cases of fluid inlet temperature change and two cases of fluid mass flow rate change cases provide a more complete understanding of the transient effectiveness method in characterizing the dynamic performance of the heat exchanger. The transient effectiveness methodology can be used as an alternative for representing the dynamic performance of the heat exchanger. It is a more effective way than using the fluid temperature results, and it contains more information, including the variation condition applied to the heat

exchanger, initial conditions and some special circumstances such as the cold fluid becoming as the hot fluid, C_{\min} fluid becoming C_{\max} fluid, and so on.

3. Characterization of a liquid cooling system using transient effectiveness

This section illustrates an example of investigating a liquid cooling system which has several heat exchanger units using the transient effectiveness method and its corresponding characteristics. Several experimental tests are conducted on a data center liquid cooling test facility and the results are reported in reference [19]. The transient effectiveness method is used to analyze the performance of heat exchangers and the dynamic performance of the entire test facility. The transient effectiveness method provides an analyzing method for investigating and characterizing the transient performance of heat exchangers which are working in the cooling and heating systems with multiple coupled heat transfer loops, in which multiple heat exchanger units are used.

3.1. Description of the test facility and experimental test scenarios

Figure 9 shows the liquid cooling chiller-less data center test facility designed by IBM. Basically the entire system contains a liquid cooling server rack, a liquid to liquid heat exchanger, and a dry cooler. The rack was fully populated with liquid cooled volume servers. Each server dissipates approximately 350 W. Then the total maximum rack power can reach 15 kW. There is also a side car heat exchanger contained within the rack on the side for cooling the rack circulated air. The air is recirculated inside the rack driven by server fans. The CPU and DIMM are cooled using cold plate and cold rails, which are directly attached to them. The heat captured by the rack circulated air and the liquid are then transferred to the atmosphere through the sidecar heat exchanger, the liquid-to-liquid heat exchanger, and the dry cooler. More details in terms of the description of each component and the entire test facility design are reported in references [19, 20].

Temperature sensors (T_1 – T_{10}) are located at various locations, including the inlet and outlet of each component, including the cold plates, servers, sidecar heat exchanger, buffer unit, and dry cooler, as shown in **Figure 8**. The detailed description of the sensor locations and functions, as well as the data collection and data processing, is summarized in reference [19]. Three transient test cases were designed and conducted and the detailed experimental designs for the three cases are shown in **Table 2**.

3.2. Transient effectiveness

3.2.1. Transient effectiveness calculation

The experimental data for the sidecar heat exchanger, the buffer unit, and the dry cooler for all the three cases are used to generate the transient effectiveness curves. The corresponding results are shown in **Figure 9(a)–(c)** for the buffer unit, the side card heat exchanger, and the dry cooler, respectively. In the current study, C_{\min} fluid of each heat exchanger unit is used in the current study.

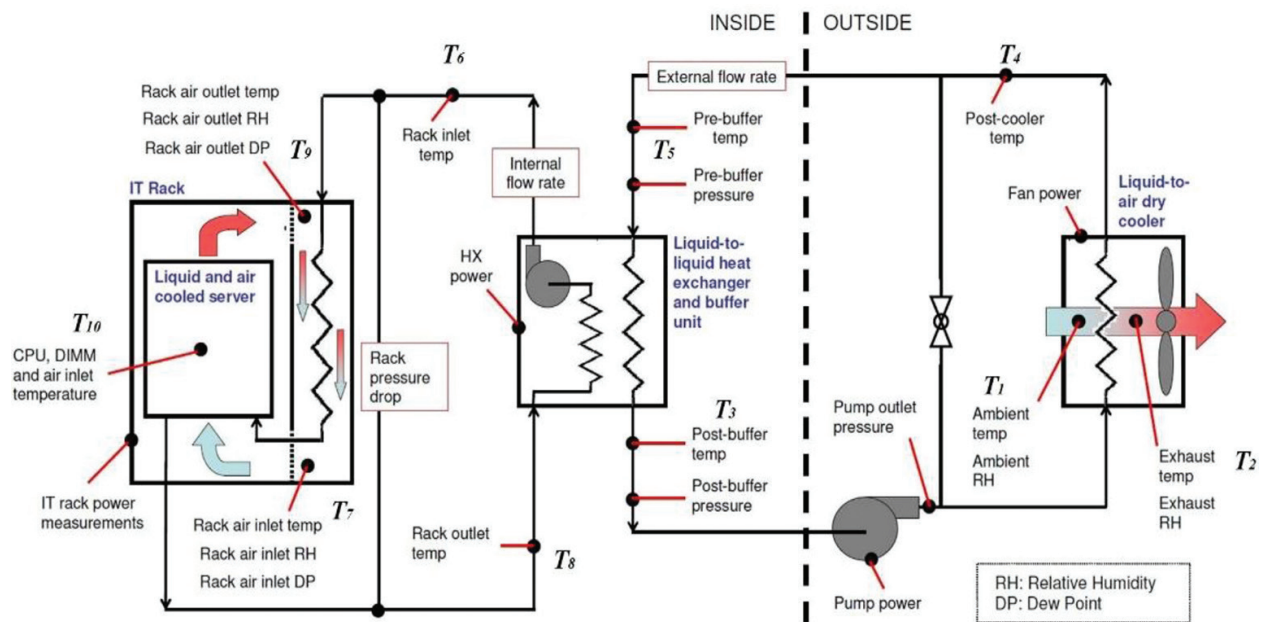


Figure 8. Schematic representation of the test facility and experimental setup.

Test cases	Server power	Internal flow rate (GPM)/water	External flow rate (GPM)/propylene glycol	Dry cooler blower fan speed set point (RPM)	Ambient air temperature (°C)
Case 1: Server power increase	Idle-Full	4	6.01	150	20.1–20.6
Case 2: Flow rate increase	Full	4–7.7	6.43	150	20.6–19.2
Case 3: Server power decrease	Full-Idle	7.7	6.43	150	19.2–18.2

Table 2. Transient test cases.

For the sidecar heat exchanger:

$$\varepsilon(\tau) = \frac{c_{air}(\tau) \cdot [T_{Rack\ outlet\ air}(\tau) - T_{Rack\ inlet\ air}(\tau)]}{c_{min}(\tau) \cdot [T_{Rack\ outlet\ air}(\tau) - T_{Prerack}(\tau)]} \quad (5)$$

For the buffer unit:

$$\varepsilon(\tau) = \frac{c_{internal}(\tau) \cdot [T_{Postrack}(\tau) - T_{Prerack}(\tau)]}{c_{min}(\tau) \cdot [T_{Postrack}(\tau) - T_{Prebuffer}(\tau)]} \quad (6)$$

For the dry cooler:

$$\varepsilon(\tau) = \frac{c_{air}(\tau) \cdot [T_{Ambient\ air}(\tau) - T_{Exhaust\ air}(\tau)]}{c_{min}(\tau) \cdot [T_{Ambient\ air}(\tau) - T_{Postbuffer}(\tau)]} \quad (7)$$

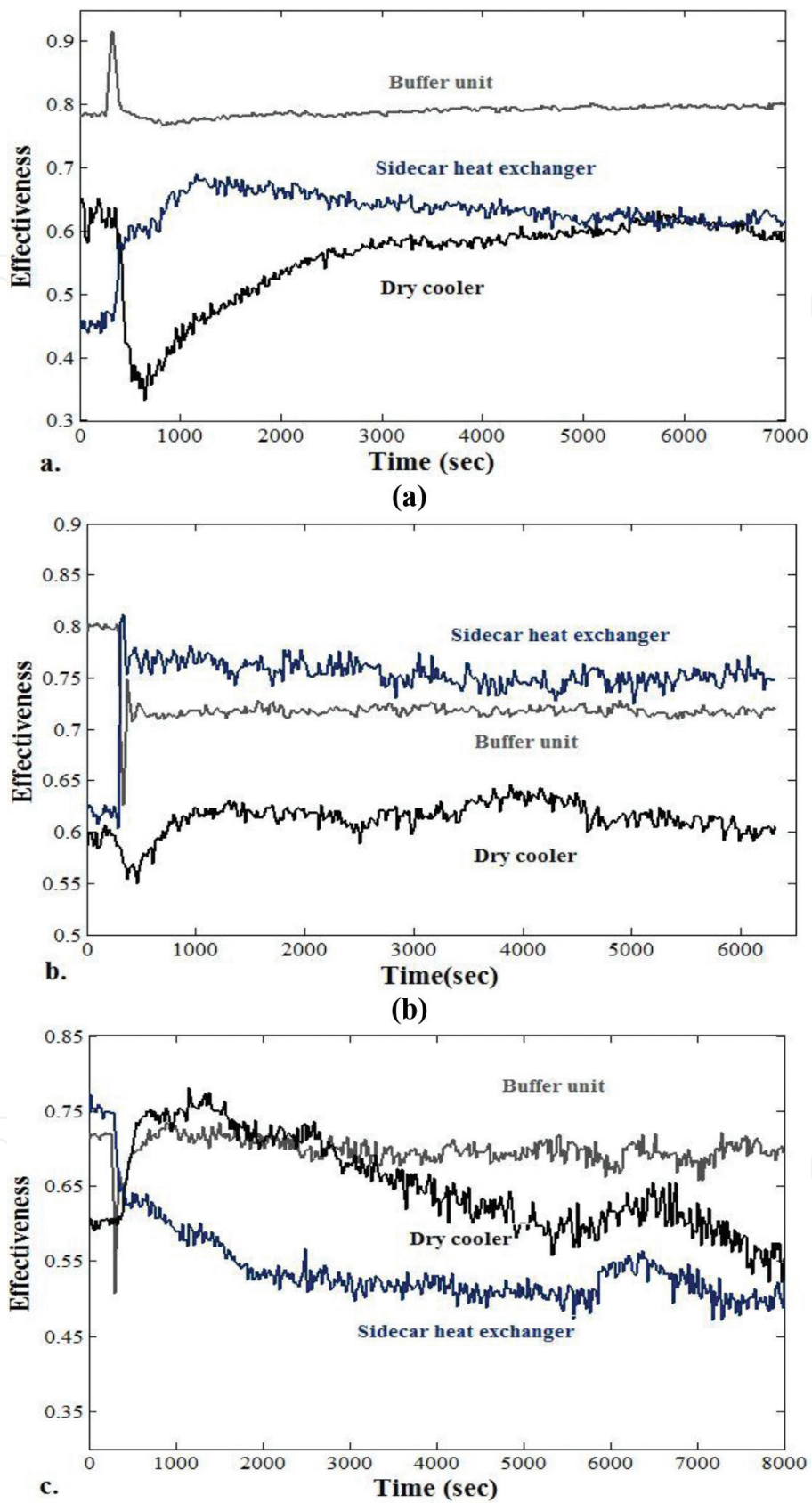


Figure 9. Transient effectiveness curves, (a) case 1; (b) case 3; and (c) case 2.

3.2.2. Transient response analysis using the transient effectiveness

The transient effectiveness for each component is plotted in **Figure 9(a)–(c)**, with the results of the three test cases. **Figure 9(a)** shows the transient effectiveness for test case 1. It can be seen by comparing the transient effectiveness curves that the transient response time of the buffer unit is very short compared to the other two heat exchangers. Since the two fluids of the buffer unit are constant, the final effectiveness is kept as the same value of 0.8. The dry cooler shows a relatively long response time, since its corresponding transient effectiveness curve takes longer time to approach a steady state. Since there is no fluid mass flow rate changes, the final steady states are the same as the initial one of 0.6. In terms of the side car heat exchanger, it can be seen that a new steady state is reached. This illustrates that the air mass flow has varied in this test case. **Figure 9(b)** shows the transient effectiveness results for case 2. In this test case, the internal fluid mass flow rate is varied. Therefore, the final steady-state values of the sidecar heat exchanger and the buffer unit are changed. In terms of the buffer unit, the effectiveness curves show a rapid response and rapidly approaches a new steady-state condition. The sidecar heat exchanger shows a similar fast response performance. The dry cooler takes much longer to reach the same steady-state condition (since the dry cooler has no fluid mass flow rate variation), compared to the other two heat exchangers. **Figure 9(c)** shows the transient effectiveness results for test case 3. Similar to test case 1, the dry cooler and the sidecar heat exchanger take longer time before they settle down and approach a steady state. The buffer unit variation time is much smaller, as shown in the curves. It is also illustrated in the transient effectiveness curves that the air flow within the server rack is varied in this test case, since the sidecar heat exchanger reaches a different final steady-state value. More analysis regarding the cause of the variation in rack air flow is presented in reference [19]. By plotting the transient effectiveness curves, the dynamic performance of each heat exchanger component and the time taken to approach a new steady state can be seen clearly. In addition, based on the characteristics of the transient effectiveness curves, more dynamic performance related to the variation applied to the heat exchanger is illustrated.

For a closed coupled system, especially when multiple heat exchanger units are used, the transient effectiveness can be used to characterize the thermal capacitance effects of each unit. **Figure 9(a)–(c)** shows that the buffer unit effectiveness reaches steady state much faster than the other two heat exchanger units. The dry cooler takes the longest time, which is seen in all three cases. This illustrates that the thermal capacitance of the buffer unit is much less than that of the dry cooler. Actually, the dry cooler is a much larger unit located outside of the building and the buffer unit is a small plate heat exchanger. The time taken for the sidecar heat exchanger to reach steady state in cases 1 and 3 is long. However, the sidecar heat exchanger takes a much shorter time in case 2. Here are some explanations: in cases 1 and 3, which involve variations in server power, the server thermal mass is involved. The impact of the thermal mass extends the time taken for the rack recirculated air and the entire rack side air dynamic to reach steady state. Then the time taken for the side card heat exchanger to reach steady state is longer in cases 1 and 3. The server thermal mass is not involved in case 2. Therefore, only the thermal capacitance of the side card heat exchanger is dominate in the transient response. Based on this analysis, it can be seen that the thermal capacitance of the sidecar heat exchanger and the buffer unit are much smaller compared with the one of the dry

cooler heat exchanger. The temperature results are collected at different locations, capturing a detailed response sequence. However, since the heat exchanger units are connected to each other using the internal loop and external loop, it is very difficult to characterize the response time of certain heat exchanger by using any temperature result. The temperature results vary during the entire test run. The transient effectiveness method provides a way to observe individual component performance, even though it is in a closed coupled system, by flitting the influence of the neighbored components. The buffer unit transient effectiveness curves have reached steady-state conditions, while the temperatures are still varying. This illustrates that the buffer unit itself has reached a steady-state thermal-exchange condition during a transient event. This can be understood as a self “steady-state” condition in a transient environment. In this condition, even though the corresponding fluid temperatures vary with time, the heat exchanger has approached a steady-state condition.

3.3. Summary

This section illustrates that the transient effectiveness can be used for characterizing the dynamic response of a closed coupled heat transfer loop, which has multiple heat exchanger units installed. It also represents the thermal capacitance impact of each component during different transient events. In addition, some detailed physical insights, which cannot be directly captured from temperature results, can be indicated by the transient effectiveness results.

4. CFD compact heat exchanger modeling

This section discusses another important application of the transient effectiveness concept and model, which can be used in developing computational fluid dynamics (CFD) compact transient heat exchanger modeling methodologies. There are two methods which are proposed in references [21, 22]. The methods can be used to model different types of heat exchangers, including a counter-flow heat exchanger and a cross-flow heat exchanger. In addition, the compact models developed can be used to model different variation scenarios, including fluid inlet temperature variation, fluid mass flow rate variation, and multiple combination variation scenarios.

4.1. Compact modeling methodology I

4.1.1. Modeling methodology development

It has been shown in previous studies that the transient effectiveness is able to characterize the dynamic response of heat exchangers. When studying heat exchanger dynamic response, the transient input can be either an inlet temperature variation or a mass flow rate variation. This case may become more complicated when considering multiple variation combination scenarios. Then the outlet temperature transient performance will be a complicated form, as shown in references [12, 23]. The transient effectiveness is correspondingly more complicated, due to the fact that the transient effectiveness is reflecting the variation in both the fluid inlet temperature and the outlet temperature. When comparing with the steady-state ε - NTU method, the first methodology was developed by extending the concept to a time-dependent effectiveness.

4.1.2. CFD compact heat exchanger model

The ε -NTU heat exchanger modeling methodology has been widely used in heat exchanger steady-state studies. This method and theoretical equations have been incorporated into most of the commercial CFD codes with a heat exchanger modeling option. For heat exchanger steady-state modeling, effectiveness performance data of the heat exchangers are used to obtain the corresponding term εC_{\min} and then the ε -NTU equation is used to represent the corresponding heat exchanger unit under certain flow rate operating conditions. The transient effectiveness concept discussed in the previous section is extended here to develop a compact transient heat exchanger model. The modeling methodology uses the transient effectiveness in the standard ε -NTU heat exchanger equation to extend the ε -NTU model to a compact transient heat exchanger form, as shown in Eq. (8). This transient effectiveness is denoted as ε_T' in the current study. By applying transient effectiveness to the equation, the transient compact model can be developed.

$$Q' = \varepsilon' C'_{\min} (T'_{h,in} - T'_{c,in}) \quad (8)$$

A CFD compact transient heat exchanger model is developed based on this transient methodology using the commercial code FloTherm [24]. The basic methodology correlates a negative linear source function as in Eq. (9) to Eq. (8) to represent the heat exchanger model. In FloTherm, the *value* and the *coefficient* can be set as transient variables for this linear heat source function. Therefore, Eq. (9) can be correlated to the transient compact heat exchanger model shown in Eq. (8). The detailed description of the FloTherm linear source model and the correlation method can be found in reference [24].

$$Q = \text{Coefficient} \times (T_{c,in} - T_{h,out}) = \text{Coefficient} \times (T_{water,in} - T_{air,out}) \quad (9)$$

4.1.3. Verification with thermal dynamic model

Thermal dynamic modeling results and the experimental test results are used as the input for calculating the transient effectiveness, and the effectiveness is then integrated into the CFD model. Then outlet temperatures predicted by the CFD compact model are compared with the thermal dynamic modeling results and experimental results. The detailed validation study is presented in reference [21]. Here a multiple variation combination case is presented as an example. It can be seen in **Figure 10** that the CFD compact modeling results are in good agreement with the thermal dynamic modeling results.

4.1.4. Verification with experimental data

In this section, this CFD compact model is verified using experimental data. The experimental tests discussed in the previous section are used. The original data are summarized in reference [19]. The transient test results, including the fluid mass flow rate and temperature variations, are incorporated into Eqs. (1a) and (1b) to calculate the transient effectiveness for the heat exchanger unit under different scenarios. Then the transient effectiveness (ε_T') is used in the CFD model. The dry cooler results are chosen as an example to discuss in this section. The detailed formulas for the transient effectiveness calculations are shown in Eq. (10).

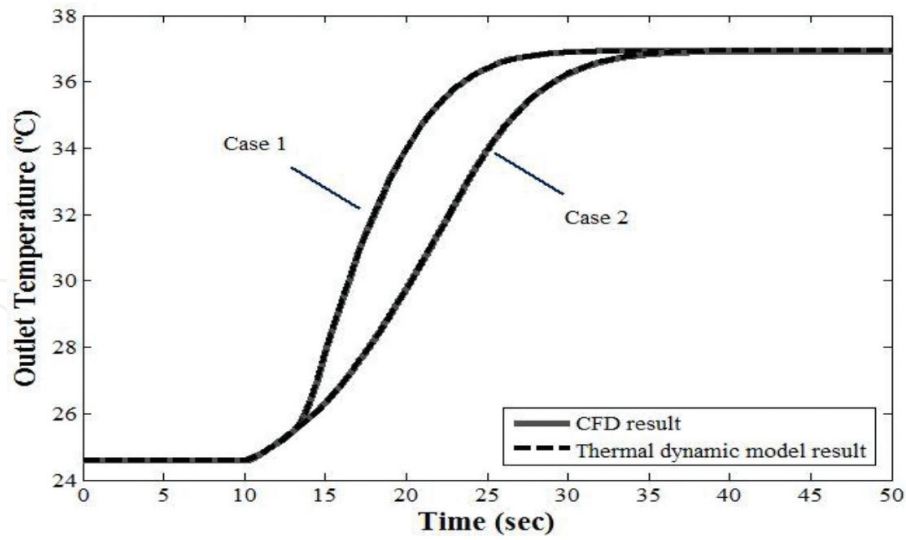


Figure 10. Hot fluid outlet temperature results, case 1: hot fluid inlet temperature step change and cold fluid mass flow rate ramp change; case 2: hot fluid inlet temperature step change and cold fluid mass flow rate step change.

For an air to liquid cross-flow heat exchanger—dry cooler:

$$\epsilon_{T'} = \frac{c_{external}(\tau) \cdot [T_{Ambient\ air}(\tau) - T_{Exhaust\ air}(\tau)]}{c_{min}(\tau) \cdot [T_{Ambient\ air}(\tau) - T_{Postbuffer}(\tau)]} \tag{10}$$

The test data discussed in Section 3 is used here for calculating the transient effectiveness of the dry cooler, and the three cases shown in Table 2 are plotted in Figure 11. The comparison results are shown in Figure 12, and the two sets of results are in good agreement.

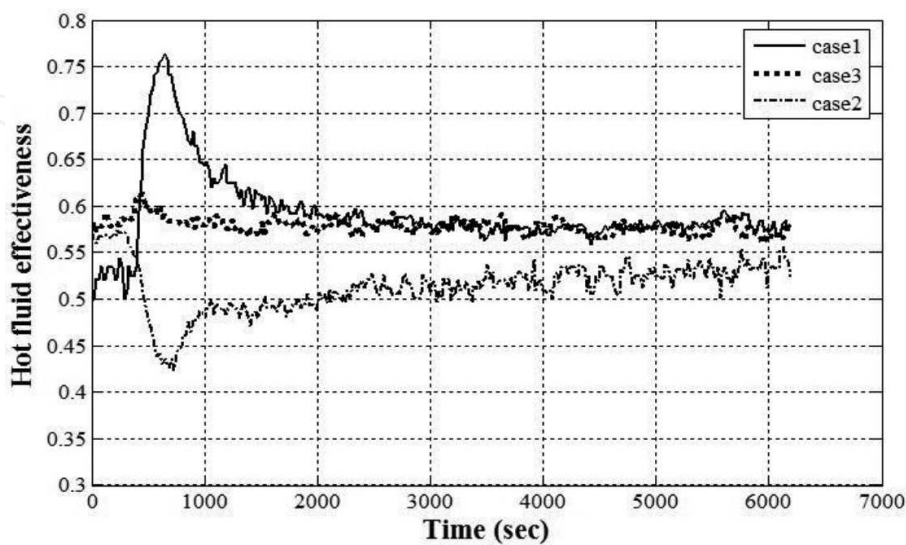


Figure 11. Hot fluid transient effectiveness in the three test cases.

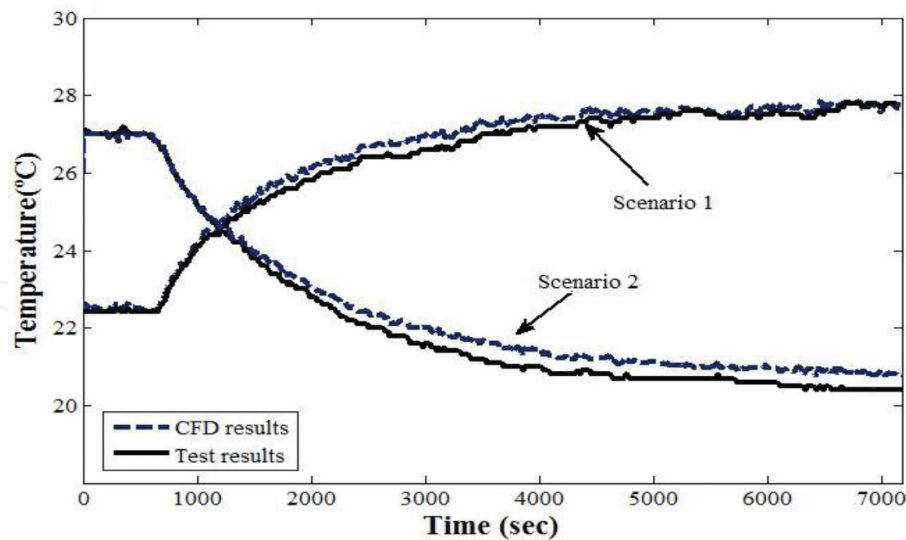


Figure 12. Comparison of the hot fluid outlet temperatures results (secondary fluid) in case 1 and case 2.

4.2. Compact modeling methodology II

The limitation of modeling methodology I is that the transient effectiveness, which used as the input for the CFD compact model, is generated based on the existing solutions from either the thermal dynamic model or experimental tests. This means that a transient effectiveness curve only represents a specific case and can only be used for modeling one certain transient case. Then the CFD model can be only used for modeling the cases with the same boundary condition, due to the limitation of the transient effectiveness used in the code. In addition, as discussed in the previous section, the transient effectiveness variation can be very complex for certain scenarios. This limitation results in the fact that this compact model may not be applied to a system level modeling work. Therefore, a derivative transient effectiveness method is developed.

4.2.1. Modeling methodology development

Eq. (11) is generated by adding the three governing partial differential equations and used as a simplified correlation in representing heat exchanger transient performance. By considering a single energy balance equation to represent the cross-flow heat exchanger using fluid inlet and out flow, Eq. (11) can be expressed in Eq. (12). The energy balance equation, together with the ε -NTU methodology, is shown in Eq. (13). Eq. (14) is then generated by substituting Eq. (13) into Eq. (12). Here, a new term $(pVc_p)_{\text{heat exchanger}}$ is introduced, which is a lumped thermal capacitance of the heat exchanger, including the capacitance of the heat exchanger metal and the two fluids. By lumping the thermal capacitances together, Eq. (14) is then expressed as Eq. (15). The term $T_{\text{heat exchanger}}$ represents the heat exchanger temperature, which can be understood as an averaged value of the two fluids and the heat exchanger metal. The negative sign represents a negative heat source. Eq. (15) is the governing equation of the second methodology. Eq. (16) is the expression of the fluid outlet temperature, and the hot fluid is used as an example.

$$MC \frac{\partial T_{wall}}{\partial t} + C_c^o \frac{\partial T_c}{\partial t} + C_h^o \frac{\partial T_h}{\partial t} + (m'c)_h \frac{\partial T_h}{\partial (y/L_h)} + (m'c)_c \frac{\partial T_c}{\partial (x/L_c)} = 0 \quad (11)$$

$$MC \frac{\partial T_{wall}}{\partial t} + C_c^o \frac{\partial T_c}{\partial t} + C_h^o \frac{\partial T_h}{\partial t} + (m'c)_h \cdot (T_{h,out} - T_{h,in}) + (m'c)_c \cdot (T_{c,out} - T_{c,in}) = 0 \quad (12)$$

$$\dot{Q} = (m'c)_c \cdot (T_{c,out} - T_{c,in}) = (m'c)_h \cdot (T_{h,out} - T_{h,in}) = \varepsilon C_{\min} \cdot (T_{h,in} - T_{c,in}) \quad (13)$$

$$MC \frac{\partial T_{wall}}{\partial t} + C_c^o \frac{\partial T_c}{\partial t} + C_h^o \frac{\partial T_h}{\partial t} + (m'c)_h \cdot (T_{h,out} - T_{h,in}) + \varepsilon C_{\min} \cdot (T_{h,in} - T_{c,in}) = 0 \quad (14)$$

$$-\dot{Q} = -\varepsilon C_{\min} \cdot (T_{h,in} - T_{c,in}) = \dot{m}c_p(T_{h,out} - T_{h,in}) + (pVc_p)_{heat\ exchanger} \times \frac{\partial T_{heat\ exchanger}}{\partial t} \quad (15)$$

$$T_{h, out} = \frac{-\varepsilon C_{\min} \cdot (T_{h,in} - T_{c,in}) - (pVc_p)_{heat\ exchanger} \times \frac{\partial T_{heat\ exchanger}}{\partial t}}{(\dot{m}c_p)_h} + T_{h, in} \quad (16)$$

4.2.2. CFD compact heat exchanger model

In reference [22], a CFD compact model is realized in the commercial CFD code FloTherm using methodology II. The detailed procedure regarding the model development is presented in reference [22]. The heat exchanger is modeled using a linear heat source module, as shown in Eq. (9), and server solid blocks, which are used to represent the thermal capacitance. Two heat source modules are used to represent the supply fluid inlet temperature and mass flow rate. The user is able to manipulate the parameters in the linear heat source module and material setting in the solid rods module to correlate it to the governing equation (Eq. (15)) of methodology II.

4.2.3. Model verification

It was mentioned that the lumped capacitance term is dominated by the capacitance of the heat exchanger coil and the two fluids, as well as their corresponding weight. For modeling verification purposes, a method was used to adjust the estimated thermal properties initially considered in the model, instead of deriving the actual lumped capacitance value. A method for lumping the three capacitance terms is a comprehensive study, which requires developing a complex physical correlation. In addition, it may vary from case to case. Basically, when using a lumped capacitance value, it should have the same impact on the heat exchanger transient response. Therefore, the curve adjustment method was used. The detailed procedure for adjusting the curve is presented in reference [22].

4.2.3.1. Inlet temperature variation scenario

The inlet temperature variation case is considered in this section, and the fluid mass flow rate is set to a constant value. For the cross-flow heat exchanger model considered in this work, the hot fluid is modeled as the supply fluid and as the C_{\min} fluid. Based on Eq. (17), the variation in the

fluid inlet temperature either T_h and/or T_c will impact the left side of the equation. The effectiveness and C_{\min} are constant values, since the fluid mass flow rate is set at a constant value.

$$\begin{aligned}
 -\varepsilon C_{\min} \cdot (T_{h,in} - T_{c,in}) &= -\varepsilon C_{\min} \cdot (T_{a,in} - T_{w,in}) = \dot{m}c_p(T_{a,out} - T_{a,in}) + (pVc_p)_{heat\ exchanger} \\
 &\times \frac{\partial T_{heat\ exchanger}}{\partial t}
 \end{aligned}
 \tag{17}$$

The analytical and numerical solutions of the thermal dynamic model shown in Eqs. (2)–(4) are used to verify the compact model shown in Eq. (17). A hot fluid inlet temperature step change scenario is used as an example in this section. **Figure 13** shows several sets of results, including the CFD modeling results, which are illustrated by solid lines, the analytical results presented in reference [8], which are indicated by discrete round black points, and the numerical results, which are plotted in dashed lines. The detailed information of each case is shown in the figure legend. It can be seen that the three sets of solutions are in good agreement for the case $NTU = 1.5$. It needs to be noted that axial dispersion is dismissed in both the numerical results and the analytical solution. It has been concluded in references [8, 25–27] that the primary fluid responds immediately, with no time delay to the sudden variation applied at the inlet. It also has been concluded that the axial dispersion has a clear impact on the fluid dynamic performance, when the NTU value is larger than 2. It can be seen in **Figure 13** that the CFD model results are in good agreement with the numerical solution. By comparing the two $NTU = 2$ cases (with and without axial dispersion), it can be seen that both the steady-state and transient performances of the outlet temperatures are influenced by the axial dispersion. Even for the same modeling case ($NTU = 2$), since the numerical results are used to calculate the ε or the coefficient value used in the CFD model, the CFD modeling results are different. It is seen that the CFD curve responds rapidly at the early response for the two $NTU = 2$ cases. Similar performance has been presented in reference [28].

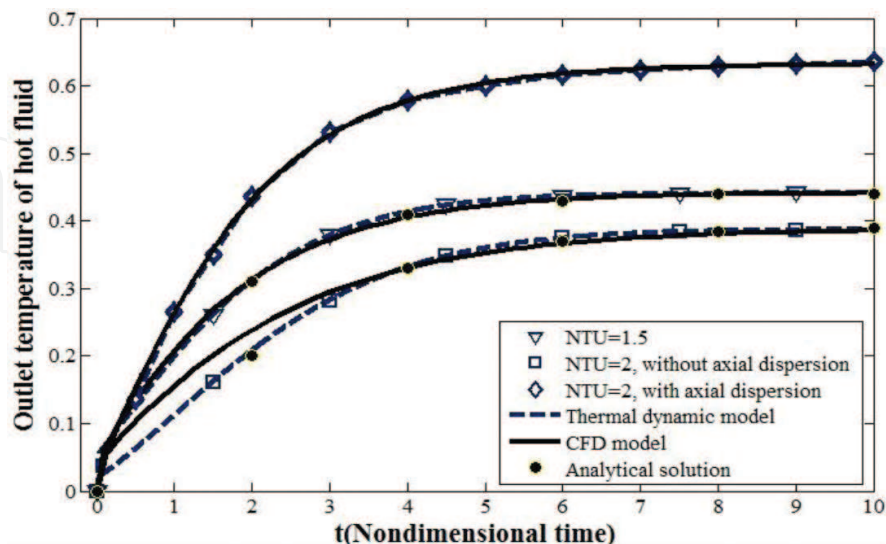


Figure 13. Comparison of the CFD modeling results with analytical and numerical solutions.

4.2.4. Fluid mass flow rate variation scenario

4.2.4.1. Mass flow rate variation-based transient effectiveness

It has been discussed in the previous section that modeling a case that involves fluid mass flow rate changes is more complicated than modeling a fluid inlet temperature variation, due to the changing in the heat transfer coefficient. Therefore, the impact of the fluid mass flow rate variation on the heat transfer coefficient should be considered. In this section, both the hot fluid and the cold fluid inlet temperatures are considered as constant. In Eq. (18), ε'_m is defined as a time-dependent variable and it represents the effectiveness changes due to fluid mass flow rate variations. The term C_{\min} is also a variable in the cases that the C_{\min} fluid mass flow rate changes.

$$-\varepsilon'_m C_{\min} \cdot (T_{h,in} - T_{c,in}) = -\varepsilon'_m C_{\min} \cdot (T_{a,in} - T_{w,in}) = \dot{m}c_p(T_{a,out} - T_{a,in}) + (pVc_p)_{heat\ exchanger} \times \frac{\partial T_{heat\ exchanger}}{\partial t} \quad (18)$$

It is important for modeling the heat exchanger transient response to correctly characterize the effectiveness due to variations in the fluid mass flow rate, and in the corresponding heat transfer coefficient. Based on the steady-state ε - NTU results, different steady-state mass flow rates and heat transfer coefficients govern the NTU values. Thus, the ε value changes due to the variation of NTU . This concept is extended to a “mass flow rate variation based” transient effectiveness. Due to the mass flow rate variation, the heat transfer coefficient changes are denoted by the NTU' value in Eq. (19). In addition, mass flow rate variations lead to changes in the heat capacity rate ratio (E'), as in Eq. (20). The detailed mathematical procedure is presented in reference [22]. Then the “mass flow rate based transient effectiveness (ε'_m)” concept is defined by extending the theoretical steady-state correlation of ε and NTU to the transient case. The theoretical steady-state correlations are shown in Eqs. (21) and (23) for a cross-flow heat exchanger and for a counter-flow heat exchanger, respectively. By integrating the NTU' and E' equations (Eqs. (19) and (20)), the mass flow rate variation-based transient effectiveness can be expressed as Eqs. (22) and (24). They are designated as the ε - NTU transient theoretical correlations. The transient theoretical correlations are used to calculate the corresponding mass flow rate based transient effectiveness under the corresponding mass flow rate variations for the CFD heat exchanger models.

$$NTU' = \frac{(mc_p)_{\min}}{(m'c_p)_{\min}} \cdot r_c^\beta \cdot \frac{(r_h^\beta + R \cdot r_h^\beta)}{r_c^\beta + R \cdot r_h^\beta} \cdot NTU \quad (19)$$

$$E' = \frac{(m'c_p)_h}{(m'c_p)_c} = \frac{r_h}{r_c} E \quad (20)$$

For a unmixed-unmixed cross-flow heat exchanger

$$\varepsilon = 1 - \exp \left\{ \frac{NTU^{0.22}}{E} [\exp(-E \cdot NTU^{0.78}) - 1] \right\} \quad (21)$$

$$\varepsilon'_m = 1 - \exp \left\{ \frac{NTU^{0.22}}{E} \left[\exp \left(-E \cdot NTU^{0.78} \right) \right] \right\} \quad (22)$$

For a counter cross-flow heat exchanger

$$\varepsilon = \frac{1 - \exp[-NTU \cdot (1 - E)]}{1 - E' \cdot \exp[-NTU \cdot (1 - E)]} \quad (23)$$

$$\varepsilon'_m = \frac{1 - \exp[-NTU' \cdot (1 - E')]}{1 - E' \cdot \exp[-NTU' \cdot (1 - E')]} \quad (24)$$

Two methodologies have been developed based on the transient effectiveness methodology. The first transient effectiveness is the temperature-based transient effectiveness, or full transient effectiveness. The second transient effectiveness is denoted as the mass flow rate based transient effectiveness method, or partial transient effectiveness. The major difference between the two transient effectiveness models is that the partial transient effectiveness only considers the impact of the variations in the fluid mass flow rate and the corresponding heat transfer coefficient, and thermal capacitance effects are dismissed.

4.2.4.2. Verification with numerical solution of thermal dynamic model

An example is selected here to perform the CFD compact model verification in modeling fluid mass flow rate changes. A set of numerical solutions for the thermal dynamic models are used. Two variation cases are considered: they are a ramp increase in the cold fluid mass flow rate, and a ramp increase in the hot fluid mass flow rate. To show the difference between the two modeling methodologies, both the full transient effectiveness and partial transient effectiveness are presented together. This difference can be seen clearly in **Figure 14**, between the two effectiveness models which are calculated using Eqs. (1a) and (22) for the same variation case. It is found that the hot fluid mass flow rate variation leads a larger difference between the two final steady states, which is not seen for the cold fluid mass flow rate variation case. One possible reason is that the hot fluid is modeled as the C_{\min} fluid. Therefore, Eq. (19) is used to calculate NTU' . Based on Eq. (19), r_h may result in a larger impact on the NTU' value than on r_c . The temperature results are plotted in **Figure 15**, and the hot fluid outlet temperatures are used to compare with the previously verified numerical solutions. It can be seen that the compact modeling results are in good agreement with the numerical solutions.

4.2.4.3. Validation with transient experimental data

Several experimental data presented in reference [29] are used to validate the modeling methodology. It needs to be mentioned that the data shown in reference [29] is for a counter-flow heat exchanger. By considering the CFD model as a black box, the counter-flow heat exchanger is modeled using the same model as the cross-flow heat exchanger, with proper modification for the model dimensions. In terms of calculating the partial transient effectiveness, Eq. (24) is used.

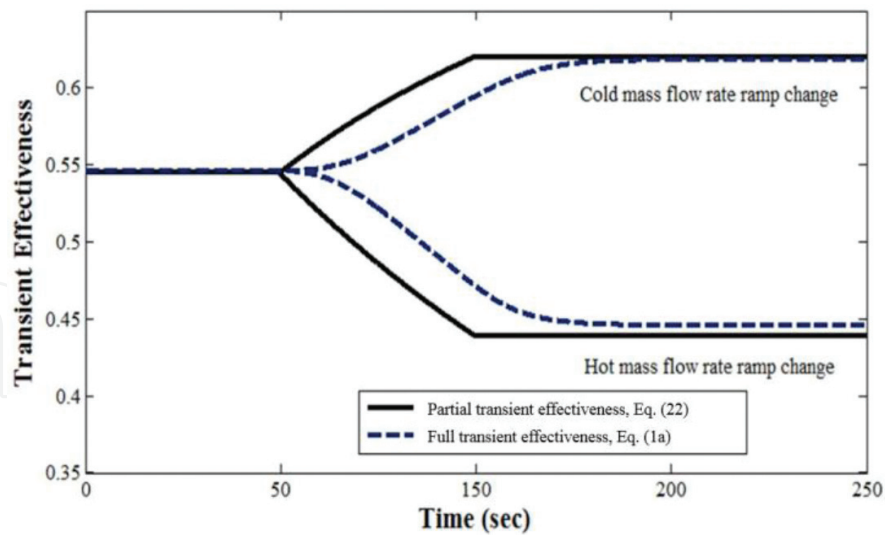


Figure 14. Transient effectiveness of the hot fluid under mass flow rate ramp change.

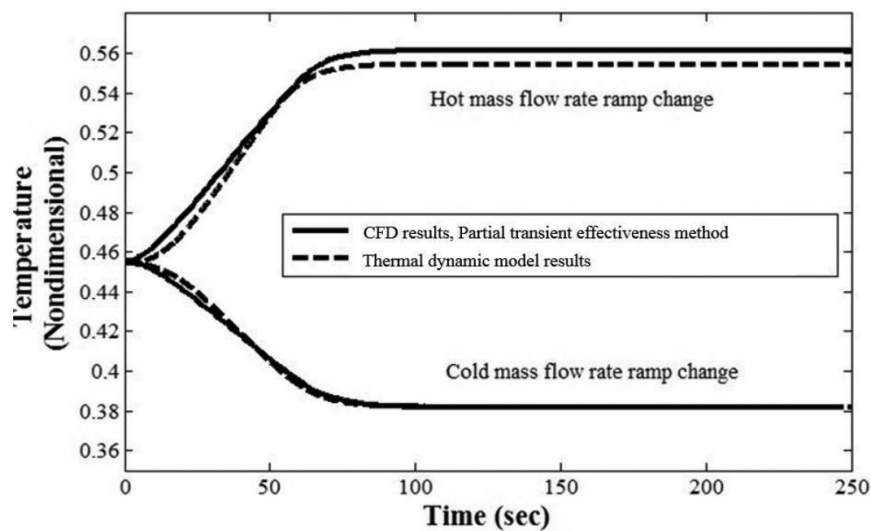


Figure 15. Outlet temperature of the hot fluid.

The mass flow rate variation magnitude was considered as $r_h = 1.56/0.45$ and applied to the hot fluid mass flow rate. The analytical solution presented in reference [29] is also plotted in the same figure. Therefore, **Figure 16** shows the experimental data, the CFD modeling results, and the analytical results. In addition, the effect of the lumped specific heat used in the current compact model is studied. Eq. (25) represents the nondimensional Peclet number. This number is used to represent the ratio of the thermal energy transported to the other fluid through convection to the energy conducted within the fluid. A small Pe_L value represents a stronger conduction effect. A large Pe_L value indicates that the impact of axial conductance is minimal. In the current CFD model, when using a relatively large heat exchanger specific heat, the axial dispersion effect can be reduced significantly. Therefore, the set point of the specific heat value has a major impact on the conductance. It can be seen in **Figure 16** that the solutions are in good agreement. When the axial dispersion impact is considered in the CFD model, the corresponding results are in good

agreement with the experimental data. When the axial dispersion impact is neglected in the CFD model, the corresponding results are in good agreement with the analytical solution. The impact of axial dispersion can be seen clearly in delaying the transient response.

$$Pe_L = \frac{UL}{k/\rho C_p} = \frac{UL \cdot \dot{m}c_p}{k} \quad (25)$$

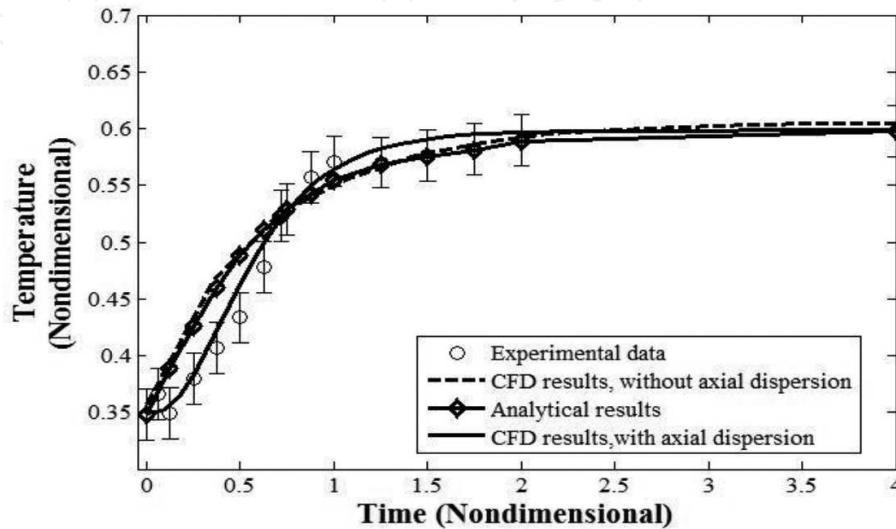


Figure 16. Fluid outlet temperature under mass flow rate step change, case 1.

4.3. Summary

In this section, the transient effectiveness concept is used to develop heat exchanger modeling methodologies. Detailed development procedures are provided. The first method is to extend the steady-state effectiveness concept to a transient concept, and the calculation of this transient effectiveness is based on the actual temperature results. This method can be used to integrate the numerical and analytical solutions and experimental data into the CFD model. The second modeling method is to extend the steady-state theoretical correlation ε - NTU to a transient correlation. This method is then used for developing CFD compact transient heat exchanger models for modeling the scenario that fluid mass flow rates change. This section provides a comprehensive summarization of the compact modeling methodology validation. Experimental data, analytical solutions, and numerical solutions are used to compare with the compact modeling results. The results show that the transient effectiveness-based CFD compact models are in good agreement with the experimental data and analytical solutions for different variation scenarios, including fluid inlet temperature changes, fluid mass flow rate changes, and combinations of multiple variations cases.

5. Conclusion

The aim of this chapter is to provide a comprehensive review of the transient effectiveness methodology for heat exchanger analysis. This chapter provides a thorough connection of all the transient effectiveness-related knowledge/work. Novel transient effectiveness methodologies

for studying heat exchanger transient characterization are introduced, and a detailed analytical, numerical, and experimental study of these models is presented. Mathematical models, analytical and numerical analysis, experimental testing, and validating studies provide a better understanding of the transient effectiveness methodology. It is shown that the transient effectiveness methodology is very useful for thermal dynamic characterization of heat exchangers and the development of compact/CFD transient models. In addition, it is found that methodology is also useful for analyzing cooling system transient experimental results.

The transient effectiveness curves represent both the heat exchanger dynamic behavior and the corresponding boundary conditions on a single curve. It depicts the heat exchanger transient response in a more comprehensive manner, when compared with outlet temperature curves.

The transient effectiveness methodology is shown to be useful for characterizing the thermal capacitance effects of the entire system, as well as each component, during transient events. The transient effectiveness curves clearly capture the transient response and the impact of thermal capacitance on each heat exchanger unit.

Two CFD compact modeling methodologies are developed and validated, namely a full transient effectiveness methodology and a partial transient effectiveness methodology. These two compact models are accurate and fast, and can be integrated into large scale models, such as system/building level models.

Acknowledgements

The authors would like to state that the majority portion of this chapter was taken from previously published work by the same group of authors.

Nomenclature

Roman letter symbols

c_p	fluid specific heat, J/kg·K
C_{wall}	specific heat of the wall of HX, J/kg·K
C_{min}	minimum capacity rate fluid
C_{max}	maximum capacity rate fluid
E	heat capacity rate ratio, $(mc_p)_h/(mc_p)_c$
D	dimension
k	thermal conductivity, W/m·K
L	length of heat exchanger, m
\dot{m}	mass flow rate, kg/s
M	mass of the wall (core) of heat exchanger, kg
NTU	number of transfer units
NTU'	time dependent NTU due to mass flow rate variation
R	conductance ratio, $(hA)_h/(hA)_c$
r	mass flow rate variation ratio, $r = \dot{m}'/\dot{m}$
T	dimensionless temperature

V	capacitance ratio
C	flow-stream capacity rate
Q/q	heat transfer rate
X, Y	dimensionless length
t	dimensionless time
RPM	revolution per minute
GPM	gallon per minute
CFM	cubic feet per minute

Dimensionless groupings

Pe_L Peclet number

Greek letter symbols

τ	time, s
ρ	density, kg/m^3
β	constant number, 0.8
ε	effectiveness
ε_T'	temperature dependent transient effectiveness/full transient effectiveness
ε_m'	mass flow rate dependent transient effectiveness/partial transient effectiveness

Subscripts

h	hot fluid
c	cold fluid
wall	coil and fin of heat exchanger
a	air
w	water
in	inlet
out/o	outlet
max	maximum
min	minimum

Author details

Tianyi Gao*, Bahgat Sammakia and James Geer

*Address all correspondence to: tgao1@binghamton.edu

SUNY Binghamton University, Binghamton, NY, USA

References

- [1] Cima, R. M., London, A. L., "Transient Response of a Two-Fluid Counter-Flow Heat Exchanger-The Gas-Turbine Regenerator," *Transactions of ASME*, Vol. 80, pp. 1169–1179, 1958.
- [2] Gao, T., Sammakia, B., Geer, J., Ortega, A., Schmidt, R., "Transient Effectiveness Characteristics of Cross Flow Heat Exchangers in Data Center Cooling Systems," In *Thermal and Thermomechanical Phenomena in Electronic Systems (ITherm)*, May 27–30, 2014 14th IEEE Intersociety Conference on, IEEE, 2014.
- [3] Gao, T., Sammakia, B., Geer, J., Ortega, A., Schmidt, R., "Dynamic Analysis of Cross Flow Heat Exchangers in Data Centers Using Transient Effectiveness Method," *IEEE Transaction of Component Packaging and Manufacturing Technology*, Vol. 4, no. 12, pp. 1925–1935, November 2014.
- [4] Dusinberre, G. M., "Calculation of Transient Temperatures in Pipes and Heat Exchangers," *Transactions of ASME*, Vol. 76, pp. 421–426, 1954.
- [5] Myers, G. E., Mitchell, J. W., Norman, R.F., "The Transient Response of Crossflow Heat Exchangers, Evaporators and Condensers," *Transactions of ASME Journal of Heat Transfer*, Vol. 89, pp. 75–80, 1967.
- [6] Romie, F. E., "Transient Response of Gas-to-Gas Crossflow Heat Exchangers with Neither Gas Mixed," *ASME Journal of Heat Transfer*, Vol. 105, pp. 563–570, 1983.
- [7] Gvozdenac, D. D., "Analytical Solution of the Transient Response of Gas-to-Gas Crossflow Heat Exchanger with Both Fluids Unmixed," *ASME Journal of Heat Transfer*, Vol. 108, pp. 722–727, 1986.
- [8] Spiga, G., Spiga, M., "Two-Dimensional Transient Solutions for Crossflow Heat Exchangers with neither Gas Mixed," *Journal of Heat Transfer*, Vol. 109, pp. 281–286, 1987.
- [9] Chen, H. T., Chen, K. C., "Simple Method for Transient Response of Gas-to-Gas Crossflow Heat exchangers With Neither Gas Mixed," *International Journal of Heat Mass Transfer*, Vol. 34, no. 11, pp. 2891–2898, 1991.
- [10] Gao, T., Sammakia, B., Geer, J., "A Review, Comparison, and Analysis of Cross Flow Heat Exchanger Transient Modeling in the Cases Fluid Mass Flow Rate and Supply Temperature Varies," *Applied Thermal Engineering*, Vol. 84, pp. 15–26, June 2015.
- [11] Gao, T., Murray, B., Sammakia, B., "Analysis of Transient and Hysteresis Behaviors of Crossflow Heat Exchangers under Variable Fluid Mass Flow Rate for Data Center Cooling Application," *Applied Thermal Engineering*, Vol. 84, pp. 15–26, June 2015.
- [12] Gao, T., Sammakia, B., Geer, J., "Dynamic response and control analysis of cross flow heat exchangers under variable temperature and flow rate conditions," *International Journal of Heat and Mass Transfer*, Vol. 81, pp. 542–553, February 2015.

- [13] Gao, T., Sammakia, B., Murray, B., Ortega, A., Schmidt, R., "Cross Flow Heat Exchanger Modeling of Transient Temperature Input Conditions," *IEEE Transactions of Component Packaging and Manufacturing Technology*, Vol. 4, no. 11, pp. 1796 – 1807, September 2014.
- [14] Rizika, J. W., "Thermal Lags in Flowing Incompressible Fluid Systems Containing Heat Capacitors," *Transactions of ASME*, Vol. 78, pp. 1407–1413, 1956.
- [15] London, A. L., Biancardi, F. R., Mitchell, J. W., "The Transient Response of Gas-Turbine Plant Heat Exchangers-Regenerators, Intercoolers, Precoolers, and Ducting," *Transaction of ASME, Journal of Engineering For Power*, Vol. 81, Series A., pp. 443–448, 1959.
- [16] DelValle, M., Ortega, A., "Experimental characterization of the transient response of air/water cross-flow heat exchangers for Data Centers cooling systems," *Proceedings of the ASME 2015 International Technical Conference and Exhibition on Packaging and Integration of Electronic and Photonic Microsystems and ASME 2015 13th International Conference on Nanochannels, Microchannels, and Minichannels*, Paper number InterPACKICNMM2015-48375, July 6–9, 2015, San Francisco, California
- [17] Gao, T., Delvalle, M., Ortega, A., Sammakia, B., "Numerical and Experimental Characterization of Transient Effectiveness of a Water to Air Heat Exchanger in data center cooling systems," *Proceedings of the ASME 2015 International Technical Conference on Packaging and Integration of Electronic and Photonic Microsystems (InterPACK 2015)*, Paper No. InterPACK2015-48371, San Francisco, CA, July 6–9, 2015.
- [18] DelValle, M., Ortega, A., "Numerical and compact models to predict the transient behavior of cross-flow heat exchangers in data center applications," *Thermal and Thermomechanical Phenomena in Electronic Systems (ITherm)*, pp. 698–705, 2014.
- [19] Gao, T., David, M., Geer, J., Schmidt, R., Sammakia, B., "Experimental and Numerical Dynamic Investigation of an Energy Efficient Liquid Cooled Chiller-Less Data Center Test Facility," *Energy & Buildings*, Vol. 91C, pp. 83–96, March 2015
- [20] David, P. M., Iyengar, K. M., Parida, P., Simons, E. R., Schultz, M., Gaynes, M., Schmidt, R., Chainer, T., "Impact of Operating Conditions on a Chiller-less Data Center Test Facility with Liquid Cooled Servers," *In Thermal and Thermomechanical Phenomena in Electronic Systems (ITherm) 2012*, San Diego, California, 2012.
- [21] Gao, T., Sammakia, B., Geer, J., David, M., Schmidt, R., "Experimentally Verified Transient Models of Data Center Crossflow Heat Exchangers," *IMECE*, Paper number IMECE2014-36022, November 14–20, Montreal, Canada, 2014.
- [22] Gao, T., Geer, J., Sammakia, B., "Development and Verification of Compact Transient Heat Exchanger Models using Transient Effectiveness Methodologies." *International Journal of Heat and Mass Transfer*, Vol. 87, pp. 265–278, 2015.
- [23] Gao, T., Geer, J., Sammakia, B., "Nonuniform Temperature Boundary Condition Effect on Data Center Cross Flow Heat Exchanger Dynamic Performance," *International Journal of Heat and Mass Transfer*, Vol. 79, pp. 1048–1058, December 2014.

- [24] Gao, T., Sammakia B., Samadiani, E., Schmidt R., “Steady State and Transient Experimentally Validate Analysis of Hybrid Data Centers,” *Journal of Electronic Packaging*, Vol. 137, no. 2, pp. 021007-021007-12, June 2015.
- [25] Roetzel, W., Xuan, Y., *Dynamic Behavior of Heat Exchangers*, Computational Mechanics Publications, Southampton, UK: WIT Press, 1999.
- [26] Shah, R. K., Sekulic, D. P., Hoboken, *Fundamentals of heat exchanger design*, NJ: John Wiley & Sons, 2003.
- [27] Baclic, B. S., Heggs, P. J., “On the Search for New Solutions of the Single-Pass Crossflow Heat Exchanger Problem,” *International Journal of Heat and Mass Transfer*, Vol. 28, no. 10, pp. 1965–1976, 1985.
- [28] Mishra, M., Das, K. P., Sarangi, S., “Transient Behavior of Crossflow Heat Exchangers with Longitudinal Conduction and Axial Dispersion,” *Journal of Heat Transfer*, Vol. 126, pp. 425–433, 2004.
- [29] Abdelghani-Idrissi, M. A., Bagui, F., Estel, L., “Analytical and Experimental Response Time to Flow Rate Step Along a Counter Flow Double Pipe Heat Exchangers,” *International Journal of Heat and Mass Transfer*, Vol. 44, no. 19, pp. 3721–3730, 2001.